Journal of Drug Delivery Science and Technology 46 (2018) 490–497

Contents lists available at ScienceDirect

Journal of Drug Delivery Science and Technology

journal homepage: www.elsevier.com/locate/jddst

Monoacyl-phospatidylcholine based drug delivery systems for lipophilic drugs: Nanostructured lipid carriers vs. nano-sized emulsions

Martin Wolf[a], Florian Reiter[b], Thomas Heuser[c], Harald Kotisch[c], Victoria Klang[b], Claudia Valenta[a,b,*]

[a] University of Vienna, Research Platform 'Characterisation of Drug Delivery Systems on Skin and Investigations of Involved Mechanisms', Althanstraße 14, 1090, Vienna, Austria
[b] University of Vienna, Department of Pharmaceutical Technology and Biopharmaceutics, Faculty of Life Sciences, Althanstraße 14, 1090, Vienna, Austria
[c] Vienna Biocenter Core Facilities - Campus Science Support Facilities GmbH, Dr. Bohr-Gasse 3, 1030, Vienna, Austria

ARTICLE INFO

Keywords:
Monoacyl-phosphatidylcholine
Nanostructured lipid carriers
NLC
Nano-sized emulsion
Skin permeation

ABSTRACT

Monoacyl-phosphatidylcholine (MAPL) offers beneficial properties as surfactant for production of nanostructured lipid carriers (NLC). A MAPL-based NLC system was modified to evaluate the effect of different formulation parameters on the skin permeation and penetration of the incorporated lipophilic model drugs flufenamic acid and fludrocortisone acetate. Increased viscosity and increased MAPL content were investigated regarding their effect on formulation properties, physico-chemical long-term stability and skin permeation. In addition, a MAPL-based oil-in-water nano-sized emulsion was developed for the first time and investigated for comparison. Results showed high storage stability of both NLC and emulsions based on surfactant mixtures with 65% w/w of MAPL; mean particle sizes and zeta potential values remained stable over 16 weeks. Diffusion cell and in vitro tape stripping studies on porcine skin showed that these NLC systems were superior to the corresponding nano-sized emulsions in terms of skin permeation. Neither increased viscosity nor higher MAPL content proved to be an additional benefit for skin permeation of the model drugs. In conclusion, MAPL-based NLC are an interesting carrier system for lipophilic drugs irrespective of the system's viscosity and superior to corresponding nanoemulsions.

1. Introduction

Drug delivery via the dermal route may be a challenging task. Different approaches to optimise skin penetration of drugs exist; one of those is the development of tailor-made innovative carrier systems [3,21,23,34]. A substantial amount of valuable data has been reported for such systems, starting with the development of solid lipid nanoparticles in the 1990s [6,24]; and the next-generation carrier system termed nanostructured lipid carriers (NLC)[1] [22,25,26].

For the production of such carrier systems, phospholipids are a well-established alternative to synthetic emulsifiers; they are frequently employed in dermal, intravenous and oral pharmaceutical formulations [28,32,33]. A regular phospholipid molecule consists of a glycerol backbone with two fatty acid esters in position 1 and 2 and a phosphatidylcholine group in position 3. A recent study has shown the traceability of phosphatidylcholine in porcine skin by vibrational spectroscopy [35]. However, few data exists on dermal formulations based on the more hydrophilic 1-monoacyl-phosphatidylcholine (MAPL)[2], where one fatty acid ester is replaced by an hydroxyl group through enzymatic reactions [9,14]. MAPL offers interesting properties for development of colloidal carrier systems such as MAPL-based self-emulsifying drug delivery system for oral delivery [12,31].

Previous work within our group has led to interesting findings regarding the role of MAPL and total lipid content within NLC formulations [36]. An optimised formulation (NLC65, see Table 1) for the delivery of lipophilic drugs was developed by using the surfactant mixture S LPC65, which consists of roughly 65% w/w of MAPL. Several points of interest arose during this work which we address in this follow-up study.

The aim of this study was to develop different MAPL-based NLC systems and nano-sized emulsions for lipophilic drugs and to investigate differences and similarities in physico-chemical stability and skin permeation. On the one hand, we wanted to elucidate whether the skin permeation of the model drugs flufenamic acid and fludrocortisone

* Corresponding author. University of Vienna, Department of Pharmaceutical Technology and Biopharmaceutics, Faculty of Life Sciences, Althanstraße 14, 1090, Vienna, Austria.
E-mail address: claudia.valenta@univie.ac.at (C. Valenta).

[1] NLC-nanostructured lipid carriers.
[2] MAPL-monoacyl-phosphatidylcholine.

https://doi.org/10.1016/j.jddst.2018.06.010
Received 23 April 2018; Received in revised form 14 June 2018; Accepted 14 June 2018
Available online 18 June 2018
1773-2247/

Table 1
Basic composition of MAPL-based systems in % w/w and abbreviations: nanostructured lipid carriers with 65% w/w MAPL content (NLC65), NLC with increased MAPL content of 80% w/w (NLC80) and nano-sized emulsions (NE65). Blank and drug-loaded systems with either flufenamic acid or fludrocortisone acetate were produced.

Constituents	NLC65	NLC80	NE65
Surfactant	5% S LPC65	5% S LPC80	5% S LPC65
Lipid phase	2.22% olive oil	2.22% olive oil	20% olive oil
	7.77% Precirol ATO5	7.77% Precirol ATO5	–
Water	ad 100%	ad 100%	ad 100%
Model drug	1% (w/w)		
	flufenamic (*fluf*) acid or fludrocortisone acetate (*fludro*)		

acetate could be modified by increased viscosity of the original NLC65 formulation (NLC65Gel). On the other hand, we wanted to compare the original NLC65 system with a corresponding NLC system with higher MAPL content (NLC80) and a corresponding MAPL-based nano-sized emulsion (NE65). Incorporation efficiency and drug content were monitored additionally to the physico-chemical properties of the systems. For the latter, photon correlation spectroscopy[3] (PCS), pH and rheology measurements as well as cryo transmission electron microscopy[4] (cryo TEM) were employed. To investigate the impact of the modified formulation properties (modification of viscosity, MAPL content or lipid core properties) on the skin permeation of the model drugs, diffusion cell studies were performed. To confirm the results in a finite-dose experimental setup, additional in vitro tape stripping experiments using porcine ear skin were conducted.

2. Material and methods

2.1. Materials

The monoacyl-phosphatidylcholine containing phospholipid mixtures *S-LPC65* and *S-LPC80* (65% or 80% w/w MAPL content) as well as purified olive oil (Ph.Eur.) were kindly provided by Lipoid GmbH (Ludwigshafen, Germany). Precirol®-ATO5 (glyceryl distearate/glyceryl palmitostearate) was provided by Gattefossé (Nanterre Cedex, France); Carbopol® 980 was provided by Lubrizol (Wickliffe, OH, USA).

Flufenamic acid (CAS 530-78-9), fludrocortisone acetate (CAS 514-36-3), TRIS[5] trizma base (EC 201-064-4) and potassium sorbate (CAS 24634-61-5) were purchased from Sigma Aldrich (St. Louis, USA). Aqueous phosphate buffer pH 7.4 (Ph.Eur.) was composed of 2.38 g of Na_2HPO_4 x 12 H_20, 0.19 g of KH_2PO_4 and 8 g of NaCl per 1000 ml of purified water. Porcine abdominal skin and pig ears were obtained from a local abattoir (Johann Gantner GmbH, Hollabrunn, Austria). All further chemicals were of analytical reagent grade and used without further purification.

2.2. Formulation composition

The basic composition of the investigated formulations NLC65, NLC80 and NE65 is given in Table 1. Amount and nature of surfactant and lipid phase is given for comparison. The gelified NLC65Gel formulation generally exhibited similar properties as the original NLC65 system; thus, it is only described separately where necessary.

2.2.1. Production of nanostructured lipid carriers

Nanostructured lipid carriers NLC65 and NLC80 were produced as recently described [36]. The aqueous phase and the lipid phase were prepared separately by stirring them at 70 °C. Next, the phases were mixed rapidly. After 1 min of pre-homogenisation with an ultraturrax Omni 5000 (Omni International, NW Kennesaw, USA) they were subjected to ultrasound treatment of two times 10 min with a Bandelin Sonopuls MS 73 (Bandelin electronic GmbH & Co. KG, Berlin, Germany) at 70 °C to achieve a mean energy input of 30 kJ. In case of drug-loaded NLC, the drug was dissolved in the oil phase (flufenamic acid 1% w/w and fludrocortisone acetate 1% w/w).

For the gelified NLC65Gel formulations, Carbopol® 980 (0.3% w/w) and trometamol (per 1 g Carbopol/0.167 g TRIS) were added to NLC65 systems after production. Potassium sorbate (0.1% w/w) was added as a preservative.

2.2.2. Production of nano-sized emulsion

The composition of the nano-sized emulsion was based on previous work [17]. The surfactant S LPC65 was mixed with a magnetic stirring bar in the aqueous phase. Potassium sorbate (0.1% w/w) was added for preservation. Olive oil was added at 70 °C; the mixture was homogenised with an ultraturrax Omni 5000 (Omni International, USA) for 4 min. The resulting emulsion was further treated with a high pressure homogeniser Emulsiflex C3 (Avestin Inc., Ottawa, ON, Canada) preheated with boiling distilled water. The emulsion was then exposed to 1000 bar of pressure for 10 cycles under high shear stress resulting in a white-creamish liquid nano-sized emulsion[6] (NE65).

2.3. Physico-chemical characterisation and stability evaluation

The parameters of interest were measured directly after production and were monitored fortnightly over an observation period of 16 weeks. Since preliminary studies have shown that refrigerated storage led to improved physical stability of the produced systems, all placebo and drug-loaded formulations were stored in airtight containers at 8 °C.

2.3.1. Mean particle size and PDI

The mean particle size and the polydispersity index[7] (PDI) of all formulations were determined by PCS using a Zetasizer Nano ZS (Malvern Instruments, Malvern, United Kingdom) at 25 °C. Samples were diluted with freshly distilled water 1:100 (v/v) containing sodium chloride (0.01 mmol). For NLC65Gels, the samples were centrifuged (12,000 rpm, 6 min, Hermle Z323K, Wehingen, Germany) and the supernatant was analysed.

2.3.2. Zeta potential

The zeta potential[8] (ZP) of the nanoparticulate systems was determined by laser Doppler electrophoresis using a Zetasizer NanoZS (Malvern Instruments, Malvern, United Kingdom) at 25 °C. Samples were diluted with distilled water (1:100 v/v) containing sodium chloride (0.01 mmol). For NLC65Gels, the samples were centrifuged (12,000 rpm, 6 min, Hermle Z323K, Wehingen, Germany) and the supernatant was analysed.

2.3.3. pH value

The pH value of the formulations was determined at room temperature (25 °C) in regular intervals to detect chemical destabilisation using a pH meter (Orion 420 A, Thermo Scientific Orion, Waltham, Massachusetts, USA).

2.4. Cryo transmission electron microscopy

The morphology of selected formulations was analysed using cryo TEM. Samples were diluted with distilled water (1:100 v/v) containing sodium chloride (0.01 mmol) to achieve results comparable to the data

[3] PCS-photon correlation spectroscopy.
[4] cryoTEM-cryo transmission electron microscopy.
[5] TRIS-trometamol.
[6] NE-nano-sized emulsion.
[7] PDI-polydispersity index.
[8] ZP-zeta potential.

obtained by PCS. To this end, quantifoil (Quantifoil Micro Tools GmbH, Großlöbichau, Germany) holey carbon copper grids (Cu 400 mesh, Multi A; hole sizes 1–8 μm) were glow discharged for 60 s at 25 mA and loaded into a Leica EM GP grid plunger (Leica Microsystems, Wetzlar, Germany). Forceps with grids were mounted into the plunger, loaded with 4 μl of sample, pre-incubated for 30 s at 21 °C and 75% humidity and then blotted with a Whatman #1 filter paper between for 1 and 8 s and then rapidly plunged into cooled ethane at approximate −185 °C for vitrification.

Cryo samples were examined using a FEI Tecnai F30 Polara Helium transmission electron microscope (FEI (Thermo Fisher Scientific), Hillsboro, OR, USA) with a 300 kV field emission gun. The microscope was operated under low dose conditions using the software SerialEM [20] and samples were kept at liquid nitrogen temperature (approximately −190 °C) at all times. Digital images were recorded with a Gatan K2 summit direct electron detector in counting mode using a defocus of 2–6 μm, a cumulative electron dose of 25 e/A^2 distributed over 20 frames at a magnification of 23.000 fold resulting in a pixel size of 1.68 Å.

2.5. Rheological characterisation

All developed formulations were analysed for their rheological properties in a controlled-rate mode using a MCR Modular Compact Rheometer (Anton Paar, Graz, Austria) with a cone and plate device (diameter 25 mm, cone angle 2°). A controlled shear rate γ was employed while maintaining a constant temperature of 32.0 °C ± 0.2 °C during all experiments. Flow curves were recorded with increasing shear rates from 1 to 100 s^{-1} to investigate the dynamic viscosity η (in Pa·s) under shear stress. The applied amount of formulation was 0.25 ml for both blank and drug-loaded formulations. Measurements were performed at least in triplicate (n ≥ 3).

2.6. Drug content and incorporation efficiency

All drug-loaded formulations were analysed on their drug content fortnightly to monitor the chemical stability of the drug. For analysis of the drug content, 10 mg of the appropriate formulation was dissolved in 1 ml of methanol in a 2 ml Eppendorf® tube. The mixture was treated in an ultrasound water bath for 6 min, centrifuged at 12,000 rpm on a Hermle Z323K (Hermle, Wehingen, Germany) and analysed by HPLC.

The incorporation efficiency of drug loaded into the lipid core was investigated immediately after preparation of the formulations. To this end, 500 μl of the appropriate formulation was vortexed with 1.5 ml distilled water in an Amicon Ultra-4 Tube (30000 kDa Cellulose, Merck-Millipore, Darmstadt, Germany). The amount of encapsulated drug was calculated by the difference between the total amount used for preparation of the formulations and the amount of drug that remained in the aqueous phase after centrifugation [30].

2.7. In vitro skin permeation studies

In vitro skin permeation studies were performed using Franz-type diffusion cells (Permegear Inc., Hellertown, PA, USA) with a permeation area of 0.95 cm^2. As a model membrane, porcine abdominal skin was used as obtained from a local abattoir after thermal and mechanical treatment to remove hair and bristles. The skin was cut with a dermatome Aesculap GA 630 DBP (Aesculap AG (B.Braun Melsungen), Tuttlingen, Germany) set at 0.7 mm and stored at −18 °C for a maximum of six months. Porcine abdominal skin is easier to obtain and to cut with a dermatome in large quantities. It represents a good compromise when a model membrane with homogeneous properties for comparative diffusion cell experiments is required. For the more realistic tape stripping setup, porcine ear skin was employed in this study (section 2.8.)

For each experiment, the skin was thawed and cut into appropriate batches to be clamped between donor and receptor chamber. The latter was filled with phosphate buffer (pH 7.4, PhEur) as acceptor medium. An infinite dose of approximately 500 mg cm^{-2} of each investigated formulation was applied onto the skin in the donor chamber. The diffusion cells were kept in a water bath at skin surface temperature (32 °C) and stirred with magnetic bars. The entire acceptor medium was removed after 2, 4, 6, 8 and 24 h, respectively, and replaced by fresh phosphate buffer. The samples were analysed for their drug content by HPLC. Experiments were performed at least in triplicate (n ≥ 3).

2.8. In vitro skin penetration studies

The penetration behaviour of both model drugs into the stratum corneum of porcine ear skin was investigated. Penetration profiles were constructed from the results of at least eight individual tape stripping experiments for each formulation. The ears were stored at −18 °C, thawed prior to the experiments, cleaned with cold water and blotted dry. The formulations were applied on a marked area at a concentration of 2 mg cm^{-2}. After 1 h of incubation, remaining formulation was removed with a tissue and 20 Corneofix® tapes were applied consecutively to remove the superficial stratum corneum layers. The amount of adherent corneocytes was determined using the infrared densitometer SquameScan 850 A (Heiland electronic, Wetzlar, Germany). The optical pseudo-absorption of the adhesive films at 850 nm (A, in %) was used to quantify the amount of stratum corneum proteins [8,18]. The mean cumulative amount of the stratum corneum proteins removed with the tapes was used to establish the penetration depth of the model drugs in relation to the complete horny layer thickness.

2.9. HPLC analysis

The drug amount of the diffusion cell samples and tape stripping experiments were analysed by HPLC using a Perkin Elmer Series ISS-200 system with a UV diode array detector (235C, Perkin Elmer, Waltham, USA). A Nucleosil 100-5 C18 column (EC250/4, MachereyNagel, Düren, Germany) and a precolumn (CC 8/4, MachereyNagel, Düren, Germany) were employed for analysis at an oven temperature of 50 °C using an injection volume of 20 μl. For both drugs, the flow rate was set at 1 ml min^{-1}. Data analysis was performed using the TotalChrom Navigator 6.3.2.

For flufenamic acid, the mobile phase consisted of methanol/water/glacial acetic acid (80/20/1 v/v) [14]. The detection wavelength was set at 245 nm. The retention time was approximately 6 min. A calibration curve was established based on peak area measurements of diluted standard solutions ranging from 0.025 μg ml^{-1} to 25.25 μg ml^{-1} with a coefficient of determination $R^2 = 0.9994$. The limit of detection for flufenamic acid was 0.422 μg ml^{-1}. The limit of quantification was set at 0.074 μg ml^{-1}.

For fludrocortisone acetate, the mobile phase consisted of acetonitrile (40/60, v/v) [13]. The wavelength of detection was set at 240 nm. The retention time of fludrocortisone acetate was approximately 8 min. A calibration curve was established from standard solutions ranging from 0.05 μg ml^{-1} to 50.50 μg ml^{-1} with a coefficient of determination $R^2 = 0.9999$. The limit of detection was found to be at 0.016 μg ml^{-1} with a limit of quantification set at 0.112 μg ml^{-1}.

2.10. Statistical analysis

Data were analysed using the GraphPad Prism 3.0 software. Results are expressed as means of at least three experiments. Parametric data were analysed using one-way ANOVA + Tukey Post Test or the Student's t-test with $p < 0.05$ as minimum level of significance. Non-parametric data (only obtained for permeation data of flufenamic acid, section 3.4) were analysed using the Kruskal-Wallis test or the Mann-Whitney test with $p < 0.05$.

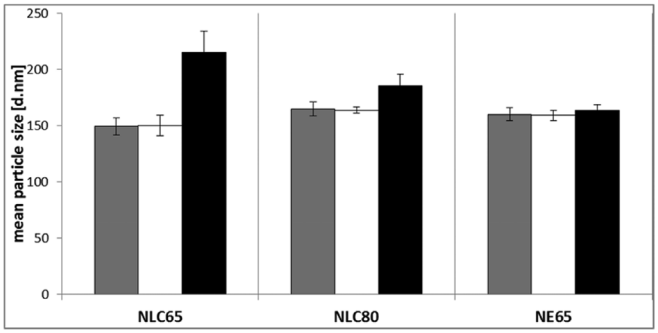

Fig. 1. Mean particle sizes in (d.nm) of NLC65, NLC80 and NE65 formulations directly after production; placebo (grey bars), flufenamic acid (white bars), fludrocortisone acetate (black bars); values are means of 3 ± SD.

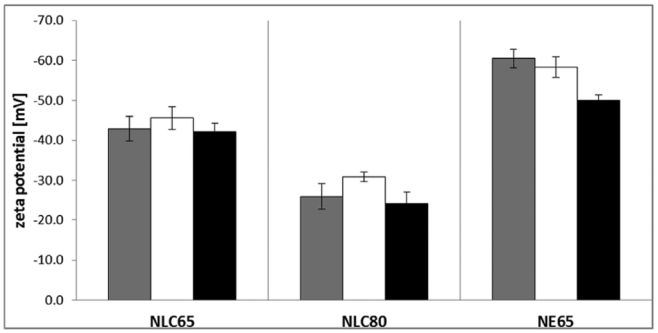

Fig. 2. Zeta potential values in (mV) from NLC65, NLC80 and NE65 formulations directly after production; placebo (grey bars), flufenamic acid (white bars), fludrocortisone acetate (black bars); values are means of 3 ± SD.

3. Results and discussion

3.1. Physiochemical characterisation and stability studies

3.1.1. Mean particle size and PDI

All developed formulations exhibited mean particle sizes of less than 220 nm. Fig. 1 shows the initial particle size values for NLC65, NLC80 and NE65. The NLC65Gel systems were mostly identical to the original NLC65, although fluctuations were observed due to polymer residues in the analysed samples (data not shown). For placebo systems, highly comparable particle size distributions were observed for all NLC systems and the NE65 emulsion ($p > 0.05$, grey bars). Incorporation of flufenamic acid did not affect the mean particle size ($p > 0.05$, white bars) while incorporation of fludrocortisone acetate led to increased particle sizes especially in case of NLC65 systems ($p < 0.05$, black bars).

In case of NLC65 formulations, mean particle sizes around 150 nm with PDI values around 0.25 were obtained for most placebo and flufenamic acid-loaded systems. Incorporation of fludrocortisone acetate led to significantly higher mean particle sizes and PDI values around 0.4 ($p < 0.05$).

In case of NLC80, particle sizes around 160 nm were observed for both placebo and flufenamic acid-containing systems. PDI values were in the same range or slightly higher than for the NLC65 counterparts (0.24–0.37). The increase in particle size caused by incorporation of fludrocortisone acetate was smaller than for NLC65 systems, but still significant ($p < 0.05$). This effect in both NLC formulations might be caused by the triterpene structure of the drug being able to influence membrane fluidity and thus affect the properties of the resulting NLC systems [1].

For Nano-sized emulsions (NE65), mean particle sizes around 160 nm were obtained for both placebo and drug-loaded formulations irrespective of the nature of the drug ($p > 0.05$). In addition, low PDI values were obtained (0.14–0.17 in all cases). It may be concluded that the different production technique resulted in superior formulations due to the employed pressure of 1000 bar [19] and/or the increased oil content proved beneficial for incorporation of the lipophilic drugs.

All formulations were monitored for their physico-chemical stability over 16 weeks; each NLC65, NLC65Gel and NE65 emulsion system exhibited stable particle size distribution and PDI value for both the placebo and drug-loaded system as well ($p > 0.05$ in all cases). In case of NLC80, good stability was observed for placebo and fludrocortisone acetate-loaded systems ($p > 0.05$) while a significant increase in particle size by 30–40 nm was observed for flufenamic acid-loaded NLC80 after 16 weeks ($p < 0.05$).

In conclusion, smaller mean particle sizes and lower PDI values were obtained for the emulsion systems. Drug incorporation appeared to be facilitated, potentially by the larger oil phase volume. For NLC, drug incorporation affected the mean particle size; nevertheless, stable formulations were obtained in all cases.

3.1.2. Zeta potential

The zeta potential is a good indicator to predict long-term stability of dermal formulations. High absolute values of more than 30 mV are desirable for electrochemical stabilisation [4]; [15].

In case of placebo NLC65 (Fig. 2), absolute values of over - 40 mV were obtained, which remained in the same range after drug incorporation ($p > 0.05$). For NLC65Gels, higher ZP values were observed than for the original NLC65 systems, potentially due to polymer residues (data not shown).

The NLC80 systems exhibited significantly lower absolute ZP values around −20 to −30 mV when compared to NLC65 (Fig. 2, $p < 0.05$ in all cases). This might be due to the higher amount of MAPL in the surfactant mixture which does not contribute to the surface charge of the produced particles [9] while the amount of potential charge carriers such as phosphatidylinositol and phospatidic acid is lower.

In case of NE65 emulsions, the highest absolute ZP values were obtained (between - 50 and - 60 mV, $p < 0.05$ when compared to corresponding NLC65), potentially due to the larger amount of incorporated oil phase and thus free fatty acids.

Regarding the storage stability of the developed systems, the ZP remained stable over the observation period of 16 weeks in all cases ($p > 0.05$). It may be concluded that all developed NLC and emulsion systems possess satisfying electrochemical stability.

3.1.3. pH value

Overall pH values for placebo formulations ranged between 4.88 ± 0.02 for NLC65, 5.16 ± 0.01 for NLC65 gels, 5.05 ± 0.02 for NLC80 particles and 6.64 ± 0.03 for NE65 emulsions. Incorporation of flufenamic acid generally led to a drop in pH by 0.5–1.0 units, while incorporation of fludrocortisone acetate only led to a minor decrease in pH.

A comparison of NLC65 with NLC65Gel formulations showed that the presence of TRIS diminished the drop in pH caused by drug incorporation due to its buffer capacity [7]. The NE65 emulsions generally exhibited the highest pH values, potentially due to the higher olive oil content.

Regarding the chemical stability of the systems, a statistically significant decrease of pH was observed for placebo and fludrocortisone acetate-loaded NLC80 and NE65 over the storage period of 16 weeks. The degradation might be caused by oxidation or hydrolysis of the involved compounds, in particular the employed lecithin mixture [11]. In case of NE65 emulsions, the decrease of pH was presumably accompanied by structural changes which led to a decrease in dynamic viscosity (section 3.3).

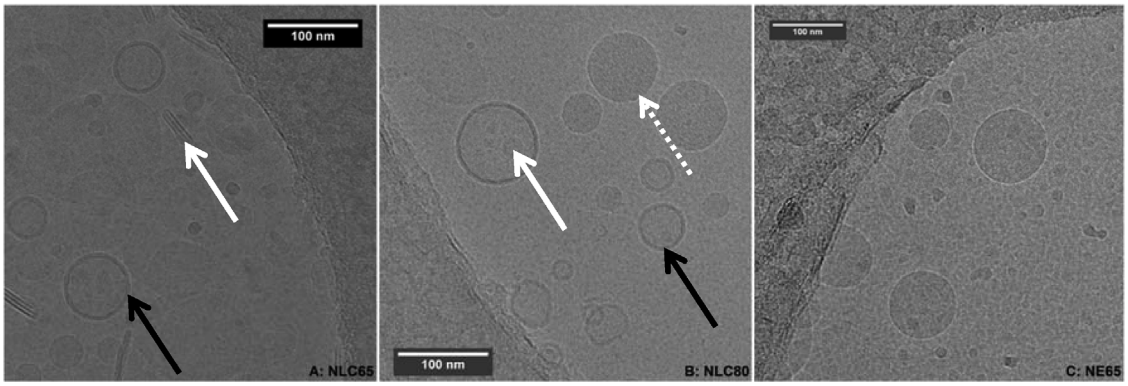

Fig. 3. Cryo TEM images of NLC65 (A, platelet-shaped NLC particles in top view (black arrow) and side view (white arrow)), NLC80 (B, platelet-shaped NLC particles in top view (black arrow), white arrow indicates adherent oil droplet on the particle surface, dotted white arrow indicates emulsified oil droplet) and NE65 (C, emulsion droplets).

3.2. Cryo transmission electron microscopy

The morphology of the NLC systems and corresponding NE65 emulsions was visualized through cryo TEM. Mean particle or droplet sizes of less than 200 nm were observed in all cases, which is in agreement with the PCS data (section 3.1.1).

In case of NLC65 and NLC80 systems, platelet-shaped particles were observed both in top and side view, which is in agreement with literature [16]; [29]. Apart from these particles, smaller bubble-like structures were observed for NLC systems; these structures might be a by-product of the ultra-sonication method and were not observed for the corresponding emulsions produced by high-pressure homogenisation (Fig. 3C). The images also suggest that there might be emulsified oil droplets present within the NLC80 systems (Fig. 3B, dotted white arrow); in general, a more heterogeneous morphology was observed for NLC than for the corresponding emulsions. This is in agreement with PCS data, which confirmed larger mean particle sizes and higher PDI values for NLC systems.

In some cases, the outer shell of the NLC particles exhibited higher contrast (Fig. 3A/B, black arrows). In addition “darker spots” were observed within the NLC structures (Fig. 3B, white arrow). Jores et al. reported that these darker structures originated from the presence of liquid oil on the surface of the “hybrid” NLC particles, which becomes visible especially in side-view of the lipid platelet. Such “nanospoon” structures with a liquid oil droplet on only one side of the platelet could be found in both NLC formulations (Fig. 3A, white arrow); they are formed due to better energetic stability [5]. No such structures were found in the nano-sized emulsion (Fig. 3C), where only one phospholipid layer was present.

3.3. Rheological properties

All developed NLC (NLC65, NLC65Gel and NLC80) showed pseudoplastic flow behaviour irrespective of their exact composition, i.e. shear thinning behaviour was observed during the experiment. For comparison, the dynamic viscosity of all investigated systems at a shear rate of $10\,s^{-1}$ at 32 °C is given in Fig. 4. In case of NLC65, a mean dynamic viscosity of 0.05 ± 0.03 Pa*s was obtained; drug incorporation led to significantly higher dynamic viscosity in case of flufenamic acid (0.20 ± 0.01, $p < 0.05$) while no notable change was observed in case of fludrocortisone acetate ($p > 0.05$).

As expected, the dynamic viscosity of the NLC65Gel was several orders of magnitude higher than that of the original aqueous NLC65 dispersions (Fig. 4). A roughly 100-fold increase of the dynamic viscosity was observed (5.36 ± 0.31, $p < 0.05$). Incorporation of flufenamic acid or fludrocortisone acetate led to significantly higher viscosity than for placebo NLC65Gels (7.43 ± 0.93 and 8.12 ± 0.35, respectively, $p < 0.05$).

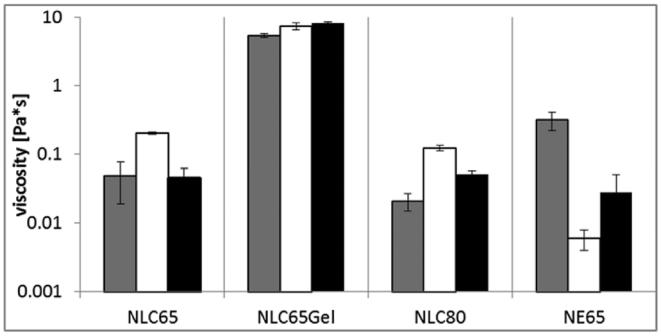

Fig. 4. Viscosity in Pa*s at 32 °C determined at a shear rate of 10 s^{-1} after production in logarithmic scale; values are given for NLC65, NLC80, NE65 as well as the gelified NLC65Gel. Placebo (grey bars), flufenamic acid (white bars) and fludrocortisone acetate (black bars); values are means of 3 ± SD.

In case of NLC80, the same trends as for NLC65 were observed, albeit with lower viscosity values. Compared to the placebo NLC80 system the viscosity of the drug-loaded NLC80 formulations were about 3-fold higher in case of fludrocortisone acetate and about 6-fold higher in case of flufenamic acid ($p < 0.01$).

The NE65 emulsions exhibited Newtonian flow behaviour. Significantly higher dynamic viscosity was observed for the placebo emulsions than for the corresponding NLC65 or NLC80 (0.31 ± 0.09, $p < 0.01$). Drug incorporation led to significantly lower dynamic viscosity in case of both flufenamic acid (0.01 ± 0.002, $p < 0.01$) and fludrocortisone acetate (0.03 ± 0.02, $p < 0.01$).

The rheological stability of the developed systems was monitored over 16 weeks. In case of NLC65, only flufenamic acid-containing systems showed a decrease in dynamic viscosity to half the original values within the first 2 weeks ($p < 0.05$) staying stable from week 4 until the end of the observation period. For all other NLC based systems no significant change in viscosity was seen.

For the NE65 emulsions, a significant decrease in viscosity by 100-fold was observed for the placebo and by 10-fold for the fludrocortisone-loaded systems between week 4 and 8 despite refrigerated storage ($p < 0.05$). Additional experiments with the placebo formulation showed an accelerated effect after 2 weeks when stored at room temperature. The initial viscosity of the flufenamic-acid containing emulsion was already 50 times lower compared to the placebo, but stayed constant for the whole observation period. Flufenamic acid might have been completely incorporated in the oily phase of the emulsion, which the drug content data confirms; the aspect of an interaction between the phospholipid bilayer membrane and the drug has been reported already [10]. However, the exact reasons for these

rheological changes remain to be clarified, especially since no physical destabilisation was visible in the PCS or laser Doppler electrophoresis measurements ($p > 0.05$).

3.4. Drug content and entrapment efficiency

Drug content and entrapment efficiency deliver important information about the successful incorporation of active pharmaceutical substances into carrier systems such as NLC.

3.4.1. Drug content

The total drug content as determined after production ranged between 84 and 101% in case of flufenamic acid and between 80 and 92% in case of fludrocortisone acetate for all systems. In case of fludrocortisone acetate, the NE65 emulsion appeared to exhibit better solubilisation capacity than the corresponding NLC, especially NLC80 (92.9 ± 3.9 vs. 79.6 ± 4.2, $p < 0.05$) due to the larger liquid oil phase.

For an estimation of the chemical stability of the developed systems, the drug content was regularly determined over an observation period of 16 weeks. Only minor fluctuations in drug content were observed for both model drugs ($p > 0.05$).

3.4.2. Entrapment efficiency

The entrapment efficiency was determined directly after production by separation of the lipophilic dispersed phase from the aqueous exterior phase of the formulations; the aqueous phase was analysed for non-encapsulated drug. The entrapment efficiency ranged between approximately 98–100% for both model drugs irrespective of the exact formulation. These high values can be attributed to the lipophilic nature of the two investigated model drugs with log P values of 5.2 in case of flufenamic acid and 1.5 for fludrocortisone acetate.

3.5. Skin permeation studies

Skin permeation experiments were employed to investigate the effect of increased viscosity, increased MAPL content and different lipid core structure on the skin diffusion of the two model drugs fludrocortisone acetate and flufenamic acid. The results are shown in Fig. 5. In general, higher cumulative permeated drug amounts were obtained for flufenamic acid, presumably due to its lower logP value when compared to fludrocortisone acetate.

In case of flufenamic acid (Fig. 5A), the optimised NLC65 formulation exhibited the highest drug permeation with a cumulative permeated amount of $53 \pm 19.73\ \mu g\ cm^{-2}$ after 24 h. This value was 2-fold higher when compared to the corresponding NLC65Gel and NE65 formulations ($30.51 \pm 8.59\ \mu g\ cm^{-2}$ and $26.19 \pm 9.23\ \mu g\ cm^{-2}$, ***$p < 0.001$, respectively) and 1.5-fold higher than for NLC80 ($38.52 \pm 13.82\ \mu g\ cm^{-2}$, **$p < 0.01$). The higher dynamic viscosity of the NLC65Gel and the higher oil content of the NE65 emulsion seemed to inhibit drug release from the formulations in the employed experimental setup; the results are in agreement with previous reports [2]; [27].

In case of fludrocortisone acetate (Fig. 5B), comparable trends were observed. The NLC65 formulation exhibited the highest cumulative amount permeated after 24 h ($5.95 \pm 2.87\ \mu g\ cm^{-2}$), followed by NLC80, NLC65Gels and NE65 emulsions ($p > 0.05$). Again, the slow diffusion from the carbopol matrix of the NLC65Gel and the entrapment of the drugs in the liquid oil compartment of the NE65 formulations appeared to slow down drug release.

3.6. Skin penetration studies

The skin penetration into the stratum corneum of porcine ear skin was investigated for both model drugs from the developed formulations.

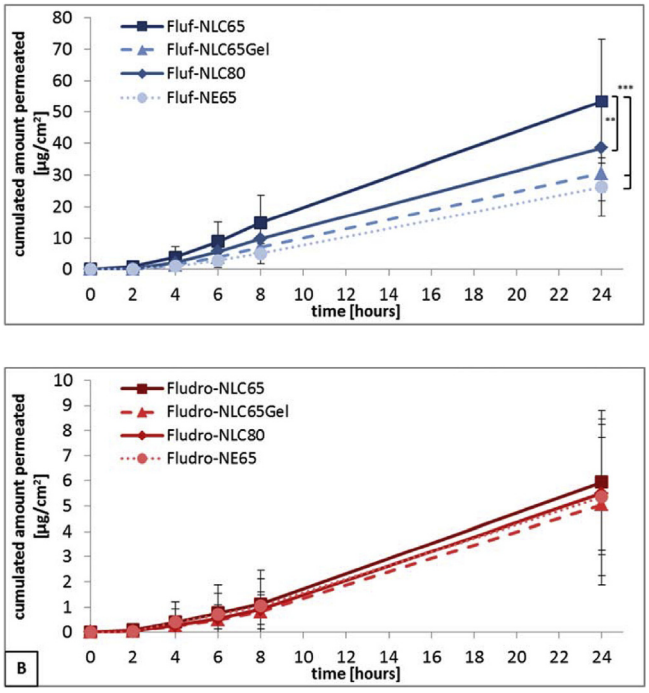

Fig. 5. Skin permeation of flufenamic acid (A) and fludrocortisone acetate (B) from the developed MAPL-based systems as determined by Franz-type diffusion cell experiments. Values are means of $n = 8 \pm SD$; statistically significant differences in determined drug amounts are marked with asterisks (**$p < 0.05$, ***$p < 0.001$).

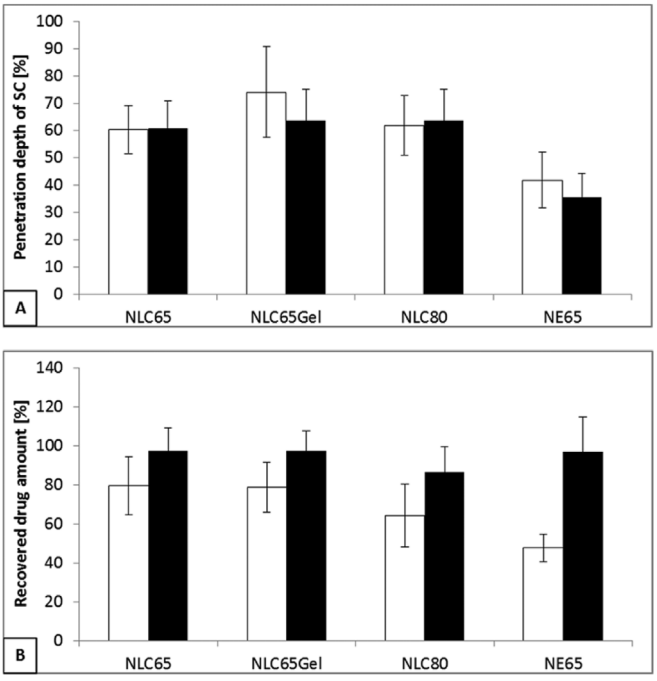

Fig. 6. Comparison of drug penetration from MAPL-based formulations into porcine ear skin as determined by in vitro tape stripping. Figure A shows the penetration depth in % of total SC thickness. Figure B depicts the cumulative drug amounts in % to the applied dose. White bars represent flufenamic acid, black bars represent fludrocortisone acetate ($n = 8$ experiments $\pm$ SD).

The skin penetration profiles were comparable for all NLC-based systems, i.e. NLC65, NLC65Gel and NLC80, for both drugs. In general, a total penetration depth of 60–75% of the entire stratum corneum was observed for flufenamic acid (Fig. 6A, white bars) and fludrocortisone

acetate (Fig. 6A, black bars). In contrast, the penetration depths achieved from NE65 emulsions were only between 35 and 40% of the entire stratum corneum and thus significantly lower than for NLC systems ($p < 0.05$ for fludrocortisone acetate). After application of the emulsion, a visible oil film remained on the skin surface, which potentially contributed to retain the incorporated lipophilic drugs on the skin surface.

When regarding the amount of penetrated drug recovered by tape stripping (Fig. 6B), the amount of flufenamic acid recovered from NLC65-based systems (NLC65 and NLC65Gel) was slightly higher than from NLC80 and significantly higher than the amount recovered from NE65 emulsions ($p < 0.05$, white bars). In contrast, the recovered drug amounts of fludrocortisone acetate were comparable for all NLC based systems and the emulsions ($p > 0.05$, Fig. 6B, black bars).

In summary, the NLC-based systems led to deeper skin penetration of both lipophilic model drugs. Regarding the penetrated drug amounts, NLC65-based systems were particularly advantageous in case of flufenamic acid; higher total drug amounts were observed when compared to the corresponding emulsion. This corresponds well with the permeation data (section 3.3).

4. Conclusions

In summary, we succeeded in producing stable MAPL-based NLC systems for two model lipophilic drugs. The developed MAPL-based NLC65 formulation yields superior in vitro skin permeation of flufenamic acid than a corresponding Nano-sized emulsion. Increased dynamic viscosity and increased MAPL content of the NLC65 system appeared to slow down the release of model drugs.

Satisfying incorporation efficiency for the model drugs was achieved. For an observation period of 16 weeks, stable drug content, mean particle sizes and zeta potential values were observed. In ongoing studies, the NLC65 system will be investigated for its performance under in vivo conditions and its effect on physiological skin parameters.

Conflicts of interest

The authors declare no conflicts of interest in this work.

Acknowledgements

The authors would like to thank Lipoid GmbH (Ludwigshafen, Germany) for providing surfactant and oil compounds. Parts of this work were financed by the Phospholipid Research Center Heidelberg and the Research platform “Characterisation of Drug Delivery Systems on Skin and Investigations of Involved Mechanisms”, University of Vienna.

References

[1] R. Abboud, C. Charcosset, H. Greige-Gerges, Tetra- and penta-cyclic triterpenes interaction with lipid bilayer membrane: a structural comparative study, J. Membr. Biol. 249 (2016) 327–338, http://dx.doi.org/10.1007/s00232-016-9871-8.

[2] V. Avasatthi, H. Pawar, C.P. Dora, P. Bansod, M.S. Gill, S. Suresh, A novel nanogel formulation of methotrexate for topical treatment of psoriasis: optimization, in vitro and in vivo evaluation, Pharmaceut. Dev. Technol. 21 (2016) 554–562, http://dx.doi.org/10.3109/10837450.2015.1026605.

[3] A. Beloqui, M.Á. Solinís, A. Rodríguez-Gascón, A.J. Almeida, V. Préat, Nanostructured lipid carriers: promising drug delivery systems for future clinics, Nanomed. Nanotechnol., Biol. Med. 12 (2016) 143–161, http://dx.doi.org/10.1016/j.nano.2015.09.004.

[4] S. Bhattacharjee, DLS and zeta potential – what they are and what they are not? J. Contr. Release 235 (2016) 337–351, http://dx.doi.org/10.1016/j.jconrel.2016.06.017.

[5] H. Bunjes, M. Drechsler, M.H.J. Koch, K. Westesen, Incorporation of the model drug ubidecarenone into Solid\rLipid nanoparticles, Pharm. Res. (N. Y.) 18 (2001) 287–293.

[6] S. Doktorovová, A.B. Kovačević, M.L. Garcia, E.B. Souto, Preclinical safety of solid lipid nanoparticles and nanostructured lipid carriers: current evidence from in vitro and in vivo evaluation, Eur. J. Pharm. Biopharm. 108 (2016) 235–252, http://dx.doi.org/10.1016/j.ejpb.2016.08.001.

[7] D. Fiorentini, L. Landi, V. Barzanti, L. Cabrini, Buffers can modulate the effect of sonication on egg lecithin liposomes, Free Radic. Res. Commun. 6 (1989) 243–250.

[8] L. Franzen, M. Windbergs, S. Hansen, Assessment of near-infrared densitometry for in situ determination of the total stratum corneum thickness on pig skin: influence of storage time, Skin Pharmacol. Physiol. 25 (2012) 249–256, http://dx.doi.org/10.1159/000339905.

[9] N. Gautschi, P. Van Hoogevest, M. Kuentz, Molecular insights into the formation of drug-monoacyl phosphatidylcholine solid dispersions for oral delivery, Eur. J. Pharmaceut. Sci. 108 (2017) 93–100, http://dx.doi.org/10.1016/j.ejps.2016.05.023.

[10] S.L. Grage, D.R. Gauger, C. Selle, W. Pohle, W. Richter, A.S. Ulrich, The amphiphilic drug flufenamic acid can induce a hexagonal phase in DMPC: a solid state 31P- and 19F-NMR study, Phys. Chem. Chem. Phys. 2 (2000) 4574–4579, http://dx.doi.org/10.1039/b003902k.

[11] M. Grit, N.J. Zuidam, W.J.M. Underberg, D.J.A. Crommelin, Hydrolysis of partially saturated egg phosphatidylcholine in aqueous liposome dispersions and the effect of cholesterol incorporation on hydrolysis kinetics, J. Pharm. Pharmacol. 45 (1993) 490–495, http://dx.doi.org/10.1111/j.2042-7158.1993.tb05585.x.

[12] S. Heuschkel, A. Goebel, R.H.H. Neubert, Microemulsions—modern colloidal Carrier for dermal and transdermal drug delivery, J. Pharmacol. Sci. 97 (2008) 603–631, http://dx.doi.org/10.1002/JPS.20995.

[13] S. Höller, C. Valenta, Effect of selected fluorinated drugs in a “ringing” gel on rheological behaviour and skin permeation, Eur. J. Pharm. Biopharm. 66 (2007) 120–126, http://dx.doi.org/10.1016/j.ejpb.2006.08.019.

[14] M. Hoppel, S. Juric, H. Ettl, C. Valenta, Effect of monoacyl phosphatidylcholine content on the formation of microemulsions and the dermal delivery of flufenamic acid, Int. J. Pharm. 479 (2015) 70–76, http://dx.doi.org/10.1016/j.ijpharm.2014.12.048.

[15] C. Jacobs, R.H. Müller, Production and characterization of a budesonide nanosuspension for pulmonary administration, Pharm. Res. (N. Y.) 19 (2002) 189–194, http://dx.doi.org/10.1023/A:1014276917363.

[16] K. Jores, W. Mehnert, M. Drechsler, H. Bunjes, C. Johann, K. Mäder, Investigations on the structure of solid lipid nanoparticles (SLN) and oil-loaded solid lipid nanoparticles by photon correlation spectroscopy, field-flow fractionation and transmission electron microscopy, J. Contr. Release 95 (2004) 217–227, http://dx.doi.org/10.1016/j.jconrel.2003.11.012.

[17] V. Klang, A. Novak, M. Wirth, C. Valenta, Semi-solid o/w emulsions based on sucrose stearates: influence of oil and surfactant type on morphology and rheological properties, J. Dispersion Sci. Technol. 34 (2012) 322–333, http://dx.doi.org/10.1080/01932691.2012.666187.

[18] V. Klang, M. Hoppel, C. Valenta, Infrared Densitometry for in Vitro Tape Stripping: Quantification of Porcine Corneocytes, (2015), http://dx.doi.org/10.1007/978-3-319-02904-7.

[19] K. Mäder, W. Mehnert, Solid lipid nanoparticles: production, characterization and applications, Adv. Drug Deliv. Rev. 47 (2001) 165–196, http://dx.doi.org/10.1016/S0169-409X(01)00105-3.

[20] D.N. Mastronarde, Automated electron microscope tomography using robust prediction of specimen movements, J. Struct. Biol. 152 (2005) 36–51, http://dx.doi.org/10.1016/j.jsb.2005.07.007.

[21] L. Montenegro, F. Lai, A. Offerta, M.G. Sarpietro, L. Micicchè, A.M. Maccioni, D. Valenti, A.M. Fadda, From nanoemulsions to nanostructured lipid carriers: a relevant development in dermal delivery of drugs and cosmetics, J. Drug Deliv. Sci. Technol. 32 (2016) 100–112, http://dx.doi.org/10.1016/j.jddst.2015.10.003.

[22] L. Montenegro, F. Lai, A. Offerta, M.G. Sarpietro, L. Micicchè, A.M. Maccioni, D. Valenti, A.M. Fadda, From nanoemulsions to nanostructured lipid carriers: a relevant development in dermal delivery of drugs and cosmetics, J. Drug Deliv. Sci. Technol. 32 (2016) 100–112, http://dx.doi.org/10.1016/j.jddst.2015.10.003.

[23] R.H. Muller, C.M. Keck, Challenges and solutions for the delivery of biotech drugs – a review of drug nanocrystal technology and lipid nanoparticles, J. Biotechnol. 113 (2004) 151–170, http://dx.doi.org/10.1016/J.JBIOTEC.2004.06.007.

[24] R.H. Müller, M. Radtke, S.A. Wissing, Solid lipid nanoparticles (SLN) and nanostructured lipid carriers (NLC) in cosmetic and dermatological preparations, Adv. Drug Deliv. Rev. 54 (2002) 131–155, http://dx.doi.org/10.1016/S0169-409X(02)00118-7.

[25] R.H. Müller, R.S. Keck, C.M., 20 Years of lipid nanoparticles (SLN & NLC): present state of development & industrial applications, Curr. Drug Discov. Technol. (2011), https://doi.org/10.2174/157016311796799062.

[26] S.-M. Pyo, R.H. Müller, C.M. Keck, Encapsulation by nanostructured lipid carriers, Nanoencapsulation Technologies for the Food and Nutraceutical Industries, Elsevier, 2017, pp. 114–137, , http://dx.doi.org/10.1016/B978-0-12-809436-5.00004-5.

[27] Y. Sangsen, P. Laochai, P. Chotsathidchai, R. Wiwattanapatapee, Effect of solid lipid and liquid oil ratios on properties of nanostructured lipid carriers for oral curcumin delivery, Adv. Mater. Res. 1060 (2014) 62–65 10.4028/www.scientific.net/AMR.1060.62.

[28] M. Schäfer-Korting, W. Mehnert, H.C. Korting, Lipid nanoparticles for improved topical application of drugs for skin diseases, Adv. Drug Deliv. Rev. 59 (2007) 427–443, http://dx.doi.org/10.1016/j.addr.2007.04.006.

[29] J.C. Schwarz, A. Weixelbaum, E. Pagitsch, M. Löw, G.P. Resch, C. Valenta, Nanocarriers for dermal drug delivery: influence of preparation method, Carrier type and rheological properties, Int. J. Pharm. 437 (2012) 83–88, http://dx.doi.org/10.1016/j.ijpharm.2012.08.003.

[30] V. Teeranachaideekul, E.B. Souto, V.B. Junyaprasert, R.H. Müller, Cetyl palmitate-based NLC for topical delivery of Coenzyme Q10-Development, physicochemical characterization and in vitro release studies, Eur. J. Pharm. Biopharm. 67 (2007)

141–148, http://dx.doi.org/10.1016/j.ejpb.2007.01.015.
[31] T. Tran, X. Xi, T. Rades, A. Müllertz, Formulation and characterization of self-nanoemulsifying drug delivery systems containing monoacyl phosphatidylcholine, Int. J. Pharm. 502 (2016) 151–160, http://dx.doi.org/10.1016/j.ijpharm.2016.02.026.
[32] P. van Hoogevest, A. Wendel, The use of natural and synthetic phospholipids as pharmaceutical excipients, Eur. J. Lipid Sci. Technol. 116 (2014) 1088–1107, http://dx.doi.org/10.1002/ejlt.201400219.
[33] M. Wacker, Nanocarriers for intravenous injection - the long hard road to the market, Int. J. Pharm. 457 (2013) 50–62, http://dx.doi.org/10.1016/j.ijpharm.2013.08.079.
[34] S. Weber, A. Zimmer, J. Pardeike, Solid lipid nanoparticles (SLN) and nanostructured lipid carriers (NLC) for pulmonary application: a review of the state of the art, Eur. J. Pharm. Biopharm. 86 (2014) 7–22, http://dx.doi.org/10.1016/j.ejpb.2013.08.013.
[35] M. Wolf, M. Halper, R. Pribyl, D. Baurecht, C. Valenta, Distribution of phospholipid based formulations in the skin investigated by combined ATR-FTIR and tape stripping experiments, Int. J. Pharm. 519 (2017) 198–205, http://dx.doi.org/10.1016/j.ijpharm.2017.01.026.
[36] M. Wolf, V. Klang, M. Halper, C. Stix, T. Heuser, H. Kotisch, C. Valenta, Monoacylphospatidylcholine nanostructured lipid carriers: influence of lipid and surfactant content on in vitro skin permeation of flufenamic acid and fluconazole, J. Drug Deliv. Sci. Technol. 41 (2017) 419–430, http://dx.doi.org/10.1016/j.jddst.2017.08.016.